Journal of Catalysis **207,** 341–352 (2002)
doi:10.1006/jcat.2002.3552, available online at http://www.idealibrary.com on IDEAL®

Evolution of Iron States and Formation of α-Sites upon Activation of FeZSM-5 Zeolites

K. A. Dubkov,* N. S. Ovanesyan,†,[1] A. A. Shteinman,† E. V. Starokon,* and G. I. Panov*,[1]

*Boreskov Institute of Catalysis, Novosibirsk 630090, Russia; and †Institute of Problems of Chemical Physics, Chernogolovka, Moscow oblast 142432, Russia

Received October 16, 2001; revised January 29, 2002; accepted January 29, 2002

Mössbauer spectroscopy *in situ* was used to study the effect of high-temperature activation on the evolution of iron introduced into a ZSM-5 zeolite matrix by various methods. The activation process (calcination in air, in vacuum, or in the presence of water vapor) was shown to cause an intensive reduction of iron, yielding two types of dinuclear Fe^{2+} complexes, which may comprise more than 60% of the total metal content. Reduced Fe^{2+} ions are stable in the presence of O_2 but are reversibly oxidized to Fe^{3+} by nitrous oxide, generating active α-oxygen species, which bring unique oxidation properties to the zeolite. After coordinative saturation by adsorbed water molecules, both iron complexes show identical Mössbauer spectra, which are close to the spectra of dinuclear iron sites in the MMO enzyme. A thorough quantitative comparison between the number of α-oxygen atoms and the number of Fe atoms involved in redox transition shows that α-sites are dinuclear complexes in which both Fe atoms are capable of α-oxygen generation.

Key Words: **FeZSM-5; Fe complexes; N_2O decomposition; α-sites; α-oxygen; monooxygenase; oxidation of benzene; phenol.**

1. INTRODUCTION

The availability of an intracrystalline micropore network of molecular size is a distinctive feature of zeolites as compared to other solids. This feature makes zeolites unique matrices, allowing stabilization of small metal complexes, which can barely form over more open surfaces. Such complexes often show unusual catalytic properties (1). One prominent example is iron complexes stabilized in the ZSM-5 matrix, called α-sites (2). According to Mössbauer data (3), iron atoms composing α-sites are in a bivalent state having a special affinity to nitrous oxide. N_2O decomposition causes Fe^{2+} transition to Fe^{3+}, producing the so-called atomic α-oxygen species, exhibiting unique oxidation features. Similar to the active oxygen of enzymes monooxygenases, α-oxygen shows remarkably high reactivity. At room temperature it oxidizes a wide range of organic molecules, including methane, selectively producing hydroxyl-containing products (4, 5). The properties of α-oxygen have been studied in many works and discussed in reviews (6, 7). These particular oxygen species participate in the direct catalytic oxidation of benzene to phenol by nitrous oxide, which is considered a potential alternative to the three-step cumene method of phenol preparation (8).

Quantum-chemical models of α-oxygen were proposed in (9, 10).

The state of active iron has been studied to a lesser extent. α-sites are known to form at the stage of high-temperature zeolite activation. At this stage Fe ions migrate from the crystalline lattice into zeolite micropores, where α-sites form (7). Mechanism details are still unclear, including such important aspects as α-sites structure and nuclearity. In the present study we focus on the answers to these questions.

For this purpose we used *in situ* Mössbauer spectroscopy combined with adsorption and catalytic measurements to study two ^{57}FeZSM-5 samples with the iron introduced by different methods. Samples were subjected to a stepwise activation of increasing intensity, accompanied by Mössbauer measurements of iron evolution combined with the measurements of α-site concentration, C_α. The idea of the work was to correlate a growing value of C_α with the different states of iron in order to identify its active form, and to reveal the α-sites composition.

2. EXPERIMENTAL

It is known that zeolites containing α-sites may be prepared by Fe addition at the synthesis stage or by its postsynthetic introduction (11). In the present work two ^{57}FeZSM-5 zeolites prepared by both methods were studied, and their characteristics are listed in Table 1.

Zeolite FeZSM-5 (A) contains 0.14 wt% Fe introduced by a postsynthetic method. For this purpose, first zeolite ZSM-5 was prepared by hydrothermal synthesis using procedures reported elsewhere (12). A silica sol (30 wt% SiO_2) and $Al_2(SO_4)_3 \cdot 18H_2O$ were used as silicon and aluminum sources. After calcination at 550°C, the zeolite was

[1] To whom correspondence should be addressed.

0021-9517/02 $35.00

TABLE 1

Characteristics of Parent ^{57}FeZSM-5 Zeolites

Zeolite	Si/Al	Iron content		Fe introduction	Crystallinity (%)	Micropore volume (cm^3/g)	A_{BET} (m^2/g)
		wt%	atom Fe/g				
FeZSM-5 (A)	45	0.14	1.5×10^{19}	$FeCl_3$, postsynthetic impregnation	100	0.17	360
FeZSM-5 (B)	21	0.31	3.2×10^{19}	$FeCl_3$, hydrothermal synthesis	95	0.15	340

converted into H-form using ammonia buffer and then impregnated with a $^{57}FeCl_3$ solution. After drying at 120°C, the resulting material was heated in vacuum at a gradual temperature increase up to 500°C. Then it was calcined in air at 550°C.

Zeolite FeZSM-5 (B) contains 0.31 wt% Fe introduced at the stage of hydrothermal synthesis. For that, a corresponding amount of $^{57}FeCl_3$ was added to the starting gel. After conversion to H-form, the zeolite was heated in a nitrogen flow at a stepwise temperature increase up to 500°C and then calcined in air at 550°C.

According to the X-ray diffraction data, both zeolites have the MFI structure with a high degree of crystallinity. They have similar micropore volumes and BET surface areas measured by low-temperature N_2 adsorption.

Activation of zeolites was performed via calcination in different media: in air (2 h), in vacuum (1 h), or in flowing helium containing 50 mol% H_2O (2 h). Activation conditions and sample designations are given in Table 2. For example, "A/air 700" stands for zeolite FeZSM-5 (A) activated by calcination in air at 700°C; "B/steam 650" stands for zeolite FeZSM-5 (B) activated in the presence of steam at 650°C.

α-Site concentration, C_α, was measured in a static vacuum setup equipped with an online mass spectrometric analyzer of the gas phase. A catalyst sample (0.3–1.0 g) was placed into a quartz microreactor and subjected to the standard pretreatment in order to normalize its initial state. Standard pretreatment involves sample heating at 550°C for 30 min in vacuum, and for 1 h in dioxygen ($P_{O_2} = 1$ Torr). Then, after reactor cooling to 250°C and O_2 replacement by N_2O, α-oxygen was loaded via N_2O decomposition, which at this temperature proceeds due to stoichiometric interaction with α-sites according to reaction [1]:

$$N_2O + (\quad)_\alpha \rightarrow (O)_\alpha + N_2. \qquad [1]$$

When all α-sites are occupied, the reaction stops. The value of C_α is estimated from the released N_2 amount (or N_2O consumed) assuming that a single oxygen atom is adsorbed on one α-site. In some cases, for higher accuracy, isotopic exchange of $^{16}O_\alpha$ with the gas-phase $^{18}O_2$ was carried out additionally. For that, the sample was cooled to 50°C, and after evacuation "heavy" molecular oxygen (95% ^{18}O) was added to the reactor. The procedures of α-site

TABLE 2

Effect of Activation on the α-Site Concentration and the Rate of Catalytic N_2O Decomposition (350°C, 0.4 Torr) over FeZSM-5 Zeolites

Sample	Activation conditions	C_α (site/g)	Rate of N_2O decomposition, W_{N_2O} (mol N_2O/g · s)	W_{N_2O}/C_α (mol N_2O/site · s)
		FeZSM-5 (A)		
1. A (parent)	No activation	2.0×10^{17}	4.0×10^{15}	0.020
2. A/air 700	Air, 700°C	9.0×10^{17}	2.0×10^{16}	0.022
3. A/air 900	Air, 900°C	1.2×10^{18}	3.8×10^{16}	0.032
4. A/vac. 900	Vacuum, 900°C	6.5×10^{18}	2.0×10^{17}	0.030
		FeZSM-5 (B)		
1. B (parent)	No activation	3.7×10^{18}	8.5×10^{16}	0.023
2. B/air 700	Air, 700°C	3.7×10^{18}	1.1×10^{16}	0.030
3. B/air 900	Air, 900°C	3.7×10^{18}	Not determ.	Not determ.
4. B/vac. 900	Vacuum, 900°C	1.3×10^{19}	3.8×10^{17}	0.029
5. B/steam 650	50% H_2O, 650°C	1.3×10^{19}	4.0×10^{17}	0.031

concentration measurements are described in detail elsewhere (13, 14).

Catalytic decomposition of N_2O with the evolution of N_2 and O_2 into the gas phase by Eq. [2],

$$N_2O \rightarrow N_2 + 1/2O_2, \qquad [2]$$

proceeds on α-sites above 300°C. We studied this reaction with the same vacuum setup which was used for α-sites measurements. Reaction was performed at 350°C ($P^{o}_{N_2O}$ = 0.4 Torr), with N_2O, N_2, and O_2 pressures being continuously monitored by mass spectrometry. The reaction rate was calculated using a graphic differentiation of initial sections of kinetic curves.

2.1. Mössbauer Measurements

Activated samples were placed into specially designed Pyrex ampoules and after connection to the vacuum setup were subjected to the same standard pretreatment which was used for the α-sites measurements. After α-oxygen was loaded and its amount was measured, the ampoules were sealed off. The Mössbauer measurements were done by mounting ampoules into the gas-flow cryostate and recording spectra at 85 K using the ^{57}Co(Rh) source. Spectra were deconvoluted into components using the least-squares method by fitting them to the Lorentzian profiles. (A deconvolution example is shown in Fig. 2.) Isomer shifts were referred to metal iron.

3. EXPERIMENT RESULTS

3.1. Effect of Activation on α-Site Concentration

α-Site concentrations in activated samples A and B are listed in Table 2. Apparently, activation conditions strongly affect the C_α value. Not only activation temperature but also its medium is of importance. For example, sample A calcination in air at 900°C results in a six-fold growth of α-site concentration (from 2.0×10^{17} to 1.2×10^{18} site/g). Calcination in vacuum at the same temperature is even more effective and provides $C_\alpha = 6.5 \times 10^{18}$ site/g.

α-Site concentration in sample B is rather high in its initial state already (3.7×10^{18} site/g). This sample is less sensitive to activation. As the calcination temperature increases to 900°C, α-site concentration remains unchanged. However, during vacuum activation at 900°C, C_α increases up to 1.3×10^{19} site/g. Steam activation appears to be particularly efficient. In this case, equally high α-site concentration is reached at a much lower temperature, such as 650°C. This fact agrees with the results reported in (15, 16), which show water vapor accelerating the hydrolysis of Si–O–Fe bonds, leading to migration of Fe atoms from the crystalline lattice into the micropore space of zeolite, thus facilitating α-site formation.

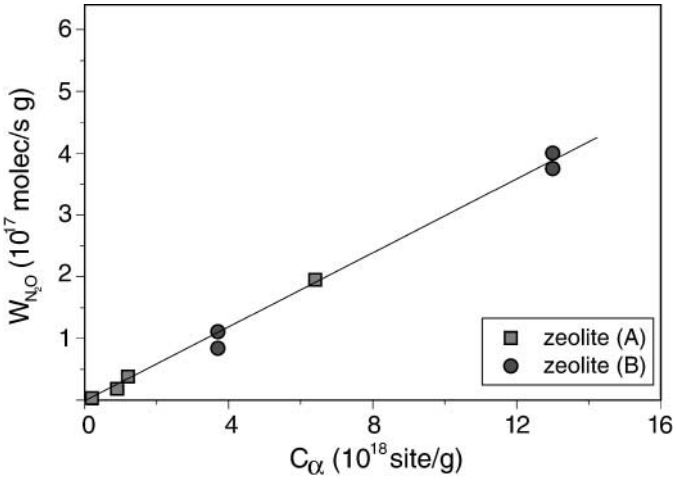

FIG. 1. Reaction rate of catalytic N_2O decomposition over FeZSM-5 (A) and FeZSM-5 (B) samples vs α-site concentration after various activations.

3.2. Catalytic Identity of α-Sites

Before starting Mössbauer measurements, it would be helpful to answer the question of whether α-sites are identical or not identical in the samples under study. The latter case would complicate our task, since it means that α-sites in different samples are represented by different iron states.

Catalytic properties are known to be very sensitive even to small changes in active sites. So, as a criterion of α-site identity we have chosen their catalytic activity in the N_2O decomposition.

Results of catalytic measurements at 350°C are presented in Table 2. In Fig. 1, plotted with the data of Table 2, one may see that rate of N_2O decomposition for samples A and B linearly depends on the α-site concentration. This indicates a constant activity of a single α-site. Indeed, if reaction rate over different samples, referred to as catalyst gram, varies within two orders of magnitude, then reaction rate of a single α-site is nearly constant and on average equals 0.025 mol of N_2O/site · s. The catalytic identity of α-sites, formed under such different conditions, is indeed a remarkable phenomenon. It allows one to conclude that most likely α-sites in different samples are represented by one or very few similar iron states.

The catalytic identity of α-sites was also reported previously for N_2O decomposition (17) and for benzene oxidation to phenol (18, 19).

3.3. Effect of Activation on the State of Iron

Mössbauer spectroscopy is one of the most informative methods for studying the state of iron. Using main spectral parameters such as isomer shift (IS) and quadruple splitting (QS), one may distinguish not only the oxidation state but also the coordination of the iron. Though spectral parameters for one and the same state may vary with the system

under study, there are several generally acknowledged principles which are used for Mössbauer spectra interpreting.

Isomer shift (also called chemical shift) characterizes s-electron density at the iron nucleons and provides information on its oxidation state. The IS values for high-spin Fe^{3+} are lower than those for high-spin Fe^{2+}. In oxygen-coordinated compounds, states with IS < 0.3 mm/s at room temperature are usually assigned to Fe^{3+} ions in tetrahedral coordination (Fe^{3+}_{Th}), while those with IS > 0.3 mm/s are assigned to octahedral coordination (Fe^{3+}_{Oh}) (20–22). Five-coordinated complexes also fall into the latter group.

Quadruple splitting is caused by the symmetry distortion in the ligand environment of the ion. The QS value for Fe^{3+} ions in ideal tetrahedrons is zero, while in distorted tetrahedrons it may attain 1.7 mm/s (23, 24). Note that high QS values ranging from 0.76 to 2.4 mm/s characterize dinuclear Fe^{3+} complexes (25, 26). Hydroxo-bridged diferric complexes have QS < 1 mm/s, as do most mononuclear high-spin ferric complexes (22). With increasing coordination numbers (e.g., upon transition from tetrahedral to octahedral coordination), the QS value for Fe^{3+} ions usually decreases, while that for Fe^{2+} ions increases (24, 27). However, for high-spin Fe^{2+} complexes, QS values cannot be used reliably as coordination number indicators (28).

At room temperature, Fe^{2+}_{Th} ions usually have IS = 0.8–1.0 mm/s and QS < 1 mm/s, while Fe^{2+} ions with coordination numbers 5 and 6 are characterized by the higher values of these parameters: IS = 1.1–1.3 mm/s, QS > 1.5 mm/s (24). On samples cooling from room temperature to 77 K, isomer shifts increase by 0.1–0.15 mm/s (29).

Mössbauer spectroscopy was repeatedly used to study iron states in zeolites of various types. These studies allow one to identify different Fe states and, in particular, to show that high-temperature treatments cause Fe removal from the crystalline lattice. In recent works (29–33), special attention was paid to dinuclear Fe complexes, since this type of complex is considered a probable active site for benzene oxidation to phenol with nitrous oxide (6), as well as for selective reduction of NO_x in excess of O_2 and H_2O (34, 35). These complexes also exhibit biomimetic features in alkane oxidation (6, 36, 37). Note that in distinction to the present work, in most previous studies zeolite samples contained a much higher iron amount, i.e., ranging from 1.4 to 8 wt% Fe.

For correct comparison of catalytic and Mössbauer data, in this work we registered spectra in glass ampoules. This allowed us to determine iron parameters under the same conditions which we applied for measurement of catalytic activity and α-site concentration.

Zeolite FeZSM-5 (A) (impregnation). Mössbauer spectra for the parent and activated samples of FeZSM-5 (A) are shown in Fig. 2. Spectra analysis reveals several states of iron, with their parameters and amounts listed in Table 3. In the parent sample iron is mainly in a trivalent oxidation state and is represented by a so-called magnetic component (54%) and doublet D1a (30%). A magnetic component (MC) appears in the spectrum as a poorly resolved sextet. In a majority of previous studies, Mössbauer spectra of Fe-containing zeolites were recorded within a narrow velocity range (mostly from −4 to +4 mm/s), which made MC contribution practically unnoticeable. With a broader velocity range, which is the case for the present work, MC contribution becomes evident, manifesting itself by a lowering of the central part of the spectra against the basic line. However, it is difficult to assign the magnetic component to a certain state of iron. Such spectral patterns may be obtained with both dispersed Fe_2O_3 phase and magnetically isolated Fe^{3+} ions located, for example, in the tetrahedral positions of a crystalline lattice (20, 38). Such signals may be also caused by the presence of FeO^+ species in the zeolite channels. These species may form at iron introduction as $FeCl_3$ followed by calcination in air (39).

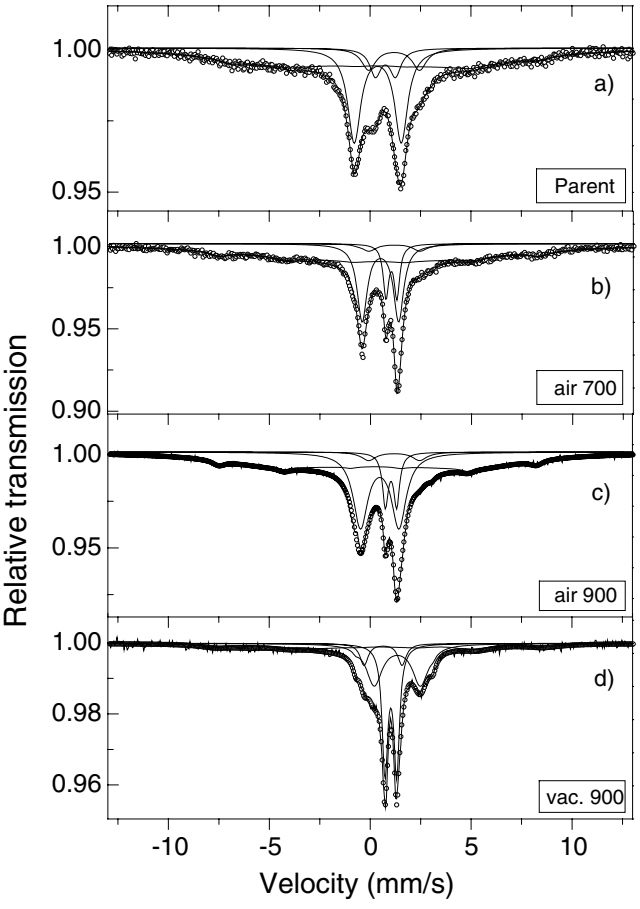

FIG. 2. Mössbauer spectra of FeZSM-5 (A) after various activations.

Doublet D1a (IS = 0.38 mm/s, QS = 2.33 mm/s) also relates to the trivalent iron. A high QS value indicates that Fe^{3+} ions are present as dinuclear μ-oxocomplexes, e.g., Fe^{3+}–O–Fe^{3+}. The formation of such oxo/hydroxo-complexes in the matrix of HZSM-5 zeolite was shown in a number of recent works (34, 40–42).

TABLE 3

Mössbauer Parameters and Amount of Iron States in FeZSM-5 (A) after Activation under Various Conditions

Sample	Subspectrum	Fe state	Spectral parameters (mm/s)		Amount of iron in the state	
			Isomer shift	Quadrupole splitting	Fraction (%)	10^{18} Fe/g
1. A (parent)	MC	Fe^{3+}	0.5	0	54	8.1
	D1a	Fe^{3+} (Oh)	0.38	2.33	30	4.5
	D2	$Fe^{2.5+}$	0.76	0.99	8	1.2
	D3	Fe^{2+} (Oh)	1.19	2.52	8	1.2
2. A/air 700	MC	Fe^{3+}	0.5	0	51	7.7
	D1	Fe^{3+} (Oh)	0.49	1.8	34	5.1
	D3	Fe^{2+} (Oh)	1.19	2.52	5	0.8
	D4	Fe^{2+} (Td)	1.04	0.54	10	1.5
3. A/air 900	MC	Fe^{3+}	0.5	0	52	7.8
	D1	Fe^{3+} (Oh)	0.47	1.9	32	4.8
	D3	Fe^{2+} (Oh)	1.19	2.52	6	0.9
	D4	Fe^{2+} (Td)	1.03	0.56	10	1.5
4. A/vac. 900	MC	Fe^{3+}	0.5	0	24	3.6
	D1	Fe^{3+} (Oh)	0.5	1.9	9	1.4
	D3	Fe^{2+} (Oh)	1.34	2.29	32	4.8
	D4	Fe^{2+} (Td)	1.02	0.58	35	5.2
5. A/vac. 900 + O_α	MC	Fe^{3+}	0.5	0	39	5.9
	D3	Fe^{2+} (Oh)	1.28	2.5	8	1.2
	D4	Fe^{2+} (Td)	1.02	0.5	12	1.8
	D5	Fe^{3+} (Oh)	0.64	1.85	26	3.9
	D6	Fe^{3+} (Th?)	0.39	0.78	15	2.3

The parent spectrum includes also two low-intensive doublets, D2 (8%) and D3 (8%), their parameters being typical for the reduced forms of iron. D3 complexes are formed by Fe^{2+} with coordination numbers of 5 or 6. D2 complexes are formed by iron in an intermediate oxidation state, $Fe^{2.5+}$. The latter may be particles of mixed valence, such as Fe^{2+}–O–Fe^{3+}, in which one electron is equally distributed over two iron site. Dimer (μ-OH) iron complexes (Fe–$(OH)_3$–Fe) of variable valence states give similar isomer shifts (43). The state with similar parameters (IS = 0.76, QS = 1.01) was observed previously for FeZSM-5 zeolite calcined in vacuum at 300–350°C (44).

Activation of FeZSM-5 (A) in air at 700 and 900°C does not affect the magnetic component but affects other states of iron. State Fe^{3+} presented as doublet D1a changes noticeably and forms a new D1 doublet. Note that a similar doublet with a comparatively high QS value shows itself as a minor component in the Mössbauer spectra of μ-oxo-bridged diiron (III) sites of several nonheme iron proteins (45). Air activation also results in the disappearance of the intermediate valence state D2. A new reduced-state D4 emerges, which may be assigned to tetrahedral ions Fe^{2+}. In case of Fe^{2+}–Y zeolite, a doublet with similar parameters (IS = 1.04, QS = 0.62, at 25°C) was assigned by Boudart and coworkers (21) to 4-coordinated $Fe^{2+}(OH)^-$ and (or) Fe^{2+}–O–Fe^{2+} ions.

Activation in vacuum at 900°C dramatically changes the Mössbauer spectrum (Fig. 2d). This relates to an intensive process of iron reduction and to a manifold increase of Fe^{2+} concentration in D3 and D4 states, which in total attains ca. 70%.

Zeolite FeZSM-5 (B) (synthesis). Mössbauer spectra of FeZSM-5 (B) zeolite, obtained by Fe introduction at the synthesis stage, are shown in Fig. 3. Spectral parameters and amounts of Fe states after various activations are listed in Table 4.

The parent zeolite contains mainly high-spin Fe^{3+}. As with zeolite A, it is represented by magnetic component MC and doublet D1 related to dinuclear complexes of Fe^{3+}(Oh). The remaining iron (10%) stays in reduced tetrahedral state Fe^{2+}(Th) as doublet D4, which in zeolite A emerges only in activated samples.

Activation in air at 700 and 900°C introduces small changes into the parent spectrum (Fig. 3, spectra b and c), while activation in vacuum as well as in steam (Fig. 3, spectra d and e) dramatically changes the spectrum. Both activations cause a considerable reduction of iron (Table 4), which exceeds 60% of the total metal amount. Reduced iron Fe^{2+} is represented by the same dinuclear states, D3 and D4, observed in FeZSM-5 (A).

Thus, despite the different ways iron is introduced into the zeolite, activation causes its intensive reduction. To a small extent, this process is observed even at calcination in air, but it is especially intensive at activation in vacuum or in steam presence. In these cases, 60–70% of iron

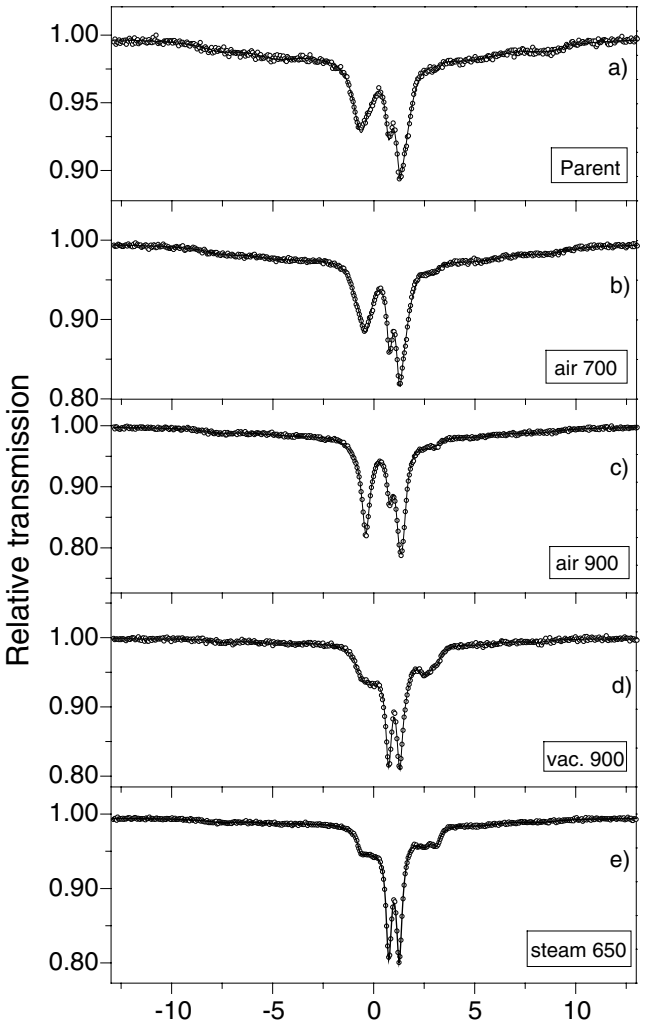

FIG. 3. Mössbauer spectra of FeZSM-5 (B) after various activations.

transforms to complexes of a bivalent state. In distinction to Fe^{2+}, which was previously observed by many authors after reductive treatments of zeolites, and which was easily reoxidized in the presence of O_2 (25, 33, 35, 46, 47), Fe^{2+} complexes in our case are remarkably stable against reoxidation by O_2. They are retained not only after the standard treatment (550°C, 1 Torr of O_2), but also after 2 h of calcination at 700°C with $P_{O_2} = 100$ Torr.

4. DISCUSSION

4.1. Active State of Iron

Iron active state is assumed to be the one composing α-sites. It means that a linear relationship should exist between the concentration of α-sites and that of active Fe species. In order to find such a relationship and to identify active iron species let us compare C_α with various states of iron detected by Mössbauer spectroscopy.

Even a cursory inspection of the results listed in Table 2 (α-site concentrations) and Tables 3 and 4 (Fe amount in various states) indicates that neither the trivalent states Fe^{3+} (MC, D1) nor the state with intermediate valence $Fe^{2.5+}$ (D2) are active. At the same time, a pronounced correlation is observed between α-site concentration and that of reduced Fe^{2+} forms. This is clearly seen from the graphic comparison in Fig. 4. With increasing C_α, concentrations of D3 and D4 complexes involving Fe^{2+} linearly increase. This fact implies that both complexes contain active iron.

Activity of complexes D3 and D4 is supported by the spectra obtained after α-oxygen loading on the vacuum-activated zeolite A (Fig. 5) as well as on vacuum-activated (not shown) and steam-activated zeolite B (Fig. 6). In both cases, O_α loading results in considerable changes of spectra related to $Fe^{2+} \rightarrow Fe^{3+}$ oxidation. It causes a strong, though incomplete, decrease in D3 and D4 concentrations (Tables 3 and 4). Concurrently, new doublets, D5 and D6, of trivalent iron emerge. After O_α desorption by heating above 300°C, these new states of Fe^{3+} disappear, and initial concentrations of D3 and D4 are restored.

Despite different Mössbauer parameters, two reduced complexes, D3 and D4, on the one hand, and two oxidized complexes, D5 and D6, on the other hand, may have similar structures. At samples hydrated by water vapor adsorbed at room temperature, each pair of complexes becomes spectrally indistinguishable (see the next section).

One may note that complexes D3 and D4 observed in this work are similar to two Fe^{2+} states observed in a ferrosilicalite by Spoto *et al.* using FTIR and UV–vis spectroscopy (46). The latter states, having different coordinative nonsaturation, also became indistinguishable at water adsorption (16).

Iron reduction at a high-temperature treatment of zeolites, performed in the absence of chemical reductant, was observed in a number of studies (3, 29, 40, 46, 48, 49) and was frequently described by the term "self-reduction." In some cases authors note that a fraction of self-reduced iron may be reoxidized only by N_2O, yielding weakly bonded and highly active oxygen species similar to O_α (31, 40, 46, 48).

It seems remarkable that, as in the case with catalytic activity (Fig. 1), linear dependencies of Fe^{2+} states versus α-site concentrations shown in Fig. 4 are common for zeolites A and B and characterize all studied samples regardless of their preparation and activation procedure.

4.2. Effect of Wet Air on the State of Iron

Earlier (3, 5), performing the Mössbauer study, we registered simpler spectra of FeZSM-5 samples. We observed only a single reduced state and a single oxidized state of active iron with the spectral parameters similar to those of iron states in methane-monooxygenase (MMO). The

TABLE 4

Mössbauer Parameters and Amount of Iron States in FeZSM-5 (B) after Activation under Various Conditions

Sample	Subspectrum	Fe state	Spectral parameters (mm/s)		Amount of iron in the state	
			Isomer shift	Quadrupole splitting	Fraction (%)	10^{18} Fe/g
1. B (parent)	MC	Fe^{3+}	0.5	0	53	17.0
	D1	Fe^{3+} (Oh)	0.49	2.1	37	11.8
	D4	Fe^{2+} (Td)	1.0	0.54	10	3.2
2. B/air 700	MC	Fe^{3+}	0.5	0	51	16.3
	D1	Fe^{3+} (Oh)	0.48	1.91	35	11.2
	D4	Fe^{2+} (Td)	1.02	0.5	14	4.5
3. B/air 900	MC	Fe^{3+}	0.5	0	55	17.6
	D1	Fe^{3+} (Oh)	0.51	1.8	30	9.6
	D3	Fe^{2+} (Oh)	1.22	2.6	5	1.6
	D4	Fe^{2+} (Td)	1.01	0.47	10	3.2
4. B/vac. 900	MC	Fe^{3+}	0.5	0	25	8.0
	D1	Fe^{3+} (Oh)	0.5	2.06	12	3.8
	D3	Fe^{2+} (Oh)	1.34	2.54	28	9.0
	D4	Fe^{2+} (Td)	1.02	0.55	35	11.2
5. B/steam 650	MC	Fe^{3+}	0.5	0	28	9.0
	D1	Fe^{3+} (Oh)	0.5	1.87	9	2.9
	D3	Fe^{2+} (Oh)	1.29	2.48	24	7.7
	D4	Fe^{2+} (Td)	1.01	0.52	39	12.5
6. B/vac. 900 + O_α	MC	Fe^{3+}	0.5	0	47	15.0
	D3	Fe^{2+} (Oh)	1.3	2.54	5	1.6
	D4	Fe^{2+} (Td)	1.01	0.52	10	3.2
	D5	Fe^{3+} (Oh)	0.62	1.61	23	7.4
	D6	Fe^{3+} (Td?)	0.39	0.80	15	4.8
7. B/steam 650 + O_α	MC	Fe^{3+}	0.5	0	30	9.6
	D3	Fe^{2+} (Oh)	1.31	2.45	16	5.1
	D4	Fe^{2+} (Th)	0.96	0.61	11	3.5
	D5	Fe^{3+} (Oh)	0.58	1.22	25	8.0
	D6	Fe^{3+} (Th?)	0.38	0.80	18	5.8

difference may be caused by the effect of atmosphere since spectra in other papers (3, 5) were recorded in air. To reveal the effect of atmosphere on the spectra patterns, in the present work, after taking spectra in ampoules, we additionally performed Mössbauer measurements in air. For the purpose ampoules were sealed off, and samples were preliminary kept for 20 h at room temperature in air saturated with water vapor. These measurements are of interest also in relation to results obtained by Boudart and coworkers (21). Using Mössbauer spectroscopy, these authors showed that Fe^{2+} ions, exchanged into zeolite Y, were nearly completely oxidized to Fe^{3+} after a 12-h contact with wet air. One cannot rule out the possibility that bivalent iron composing α-sites is also liable to slow oxidation on contact with atmosphere.

Figure 7 shows FeZSM-5 (A) spectra taken after samples contact wet air. Comparison of this figure with Fig. 2 (spectra in ampoules) reveals considerable spectra differences. Similar changes were observed also for the FeZSM-5 (B) samples (not shown). Parameters of iron states and their amounts for "air" samples A and B are listed in Tables 5 and 6. One can see that spectral parameters of magnetic component remain unaffected. In contrast, parameters of active forms of iron change considerably due to water adsorption and alteration of their coordination states. As a result, distinctions between D3 and D4 complexes of bivalent iron disappear, and they merge into a new octahedral Fe^{2+} state denoted as D-II (Tables 5 and 6). Similar changes occur with the oxidized Fe^{3+} states: D5 and D6 doublets also become indistinguishable and form a single new state, D-I. But unlike Fe^{2+}–Y (21), FeZSM-5 contacting wet atmosphere does not induce bivalent iron oxidation. We see it by comparing the concentrations of Fe^{2+} for samples in ampoules (D3 + D4, Tables 3 and 4) and in air (D-II, Tables 5 and 6). In all cases these concentrations are close.

Spectral parameters of new hydrated states indicate a dinuclear structure of Fe^{3+} complexes. As for the structure of reduced complexes, Mössbauer spectra cannot give clear indications. However, considering the reversibility of the redox iron transition as well as zeolite matrix rigidity, one may conclude that the dinuclear structure is retained for the entire catalytic cycle.

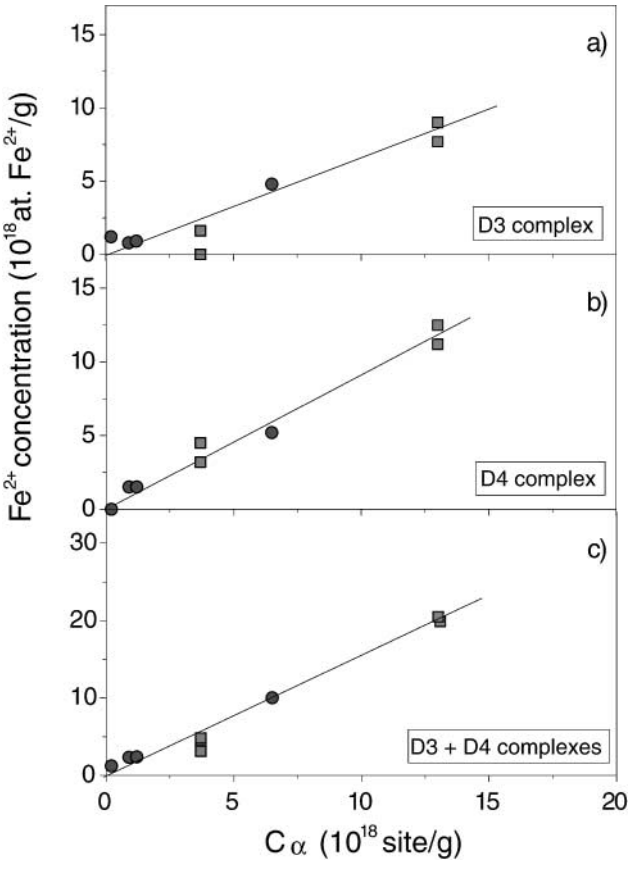

FIG. 4. Concentration of Fe^{2+} ions in complexes D3 and D4 vs concentration of α-sites after various activations: ●, FeZSM-5 (A); ■, FeZSM-5 (B).

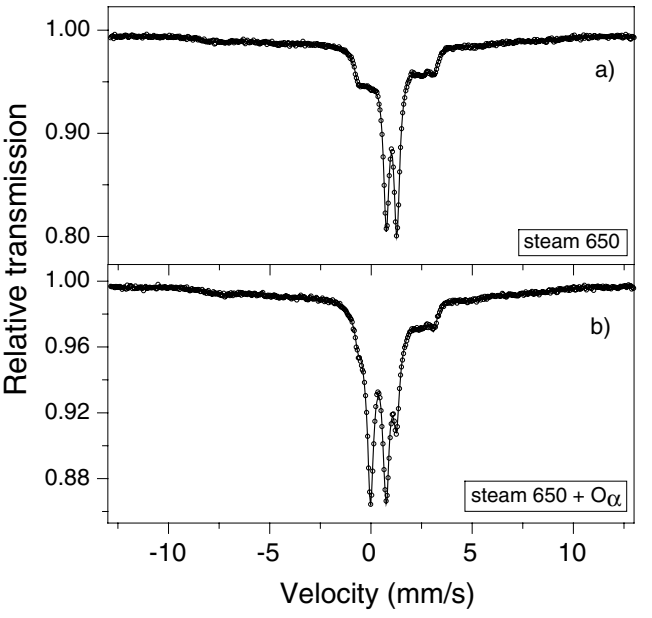

FIG. 6. Mössbauer spectra of FeZSM-5 (B) after steam activation (a) followed by α-oxygen loading (b).

It is interesting that the Mössbauer spectra of hydrated samples remarkably resembles those of dinuclear iron site in MMO. Depending on conditions, iron in MMO exists in the reduced and oxidized states. Each of these states is represented by its own doublet, with parameters listed in Table 7 (50). One may see that in both reduced and

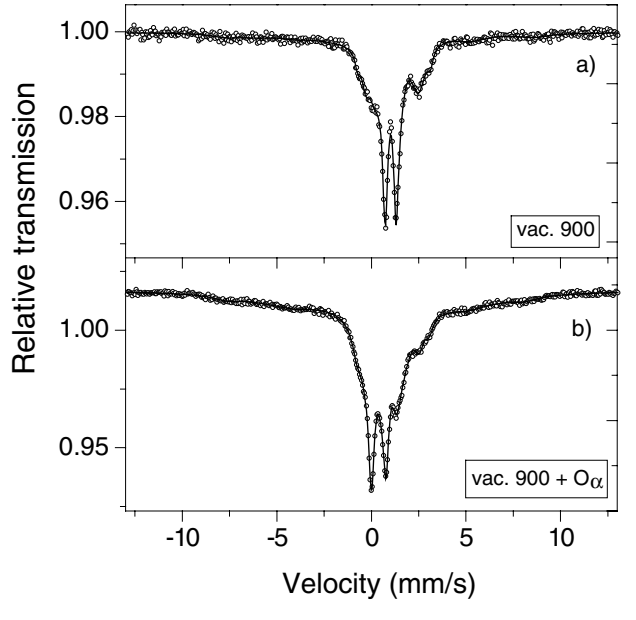

FIG. 5. Mössbauer spectra of FeZSM-5 (A) after activation in vacuum (a) followed by α-oxygen loading (b).

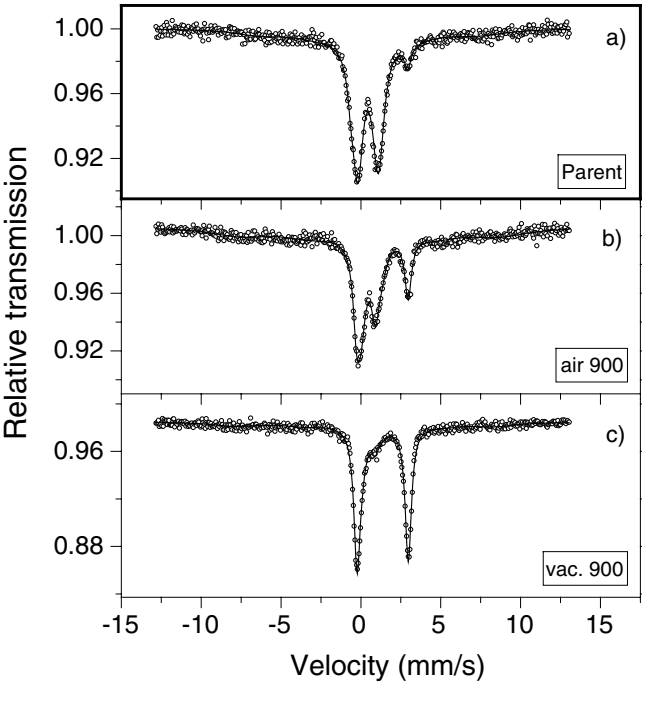

FIG. 7. Mössbauer spectra of parent and activated FeZSM-5 (A) after contacting wet air.

TABLE 5

Mössbauer Parameters and Amount of Iron States in FeZSM-5 (A) after Contacting Wet Air

Sample	Subspectrum	Fe state	Spectral parameters (mm/s)		Amount of iron in the state	
			Isomer shift	Quadrupole splitting	Fraction (%)	10^{18} Fe/g
1. A (parent)	MC	Fe^{3+}	0.5	0	47	7.1
	D-I	Fe^{3+} (Oh)	0.47	0.93	40	6.0
	D-II	Fe^{2+} (Oh)	1.35	3.26	13	2.0
2. A/air 700	MC	Fe^{3+}	0.5	0	33	5.0
	D-I	Fe^{3+} (Oh)	0.48	0.96	49	7.4
	D-II	Fe^{2+} (Oh)	1.34	3.19	18	2.7
3. A/air 900	MC	Fe^{3+}	0.5	0	34	5.1
	D-I	Fe^{3+} (Oh)	0.47	0.96	48	7.2
	D-II	Fe^{2+} (Oh)	1.34	3.19	18	2.7
4. A/vac. 900	MC	Fe^{3+}	0.5	0	16	2.3
	D-I	Fe^{3+} (Oh)	0.5	0.9	15	2.3
	D-II	Fe^{2+} (Oh)	1.36	3.21	69	10.3
5. A/vac. 900 + O_α	MC	Fe^{3+}	0.5	0	37	5.6
	D-I	Fe^{3+} (Oh)	0.47	0.96	42	6.3
	D-II	Fe^{2+} (Oh)	1.37	3.2	21	3.2

TABLE 6

Mössbauer Parameters and Amount of Iron States in FeZSM-5 (B) after Contacting Wet Air

Sample	Subspectrum	Fe state	Spectral parameters (mm/s)		Amount of iron in the state	
			Isomer shift	Quadrupole splitting	Fraction (%)	10^{18} Fe/g
1. B (parent)	MC	Fe^{3+}	0.5	0	66	21.1
	D-I	Fe^{3+} (Oh)	0.49	0.9	22	7.0
	D-II	Fe^{2+} (Oh)	1.39	3.29	12	3.8
2. B/air 700	MC	Fe^{3+}	0.5	0	62	19.8
	D-I	Fe^{3+} (Oh)	0.49	0.9	23	7.4
	D-II	Fe^{2+} (Oh)	1.38	3.27	15	4.8
3. B/air 900	MC	Fe^{3+}	0.5	0	43	13.8
	D-I	Fe^{3+} (Oh)	0.49	0.9	41	13.1
	D-II	Fe^{2+} (Oh)	1.35	3.22	16	5.1
4. B/vac. 900	MC	Fe^{3+}	0.5	0	20	6.4
	D-I	Fe^{3+} (Oh)	0.49	0.82	15	4.8
	D-II	Fe^{2+} (Oh)	1.38	3.24	65	20.8

TABLE 7

Mössbauer Parameters of Iron in MMO and FeZSM-5

System	Fe state	Spectral parameters (mm/s)		Reference
		Isomer shift	Quadrupole splitting	
MMO, Me. capsulatus (Bath)	Fe(II)–Fe(II)	1.30	3.01	50
	Fe(III)–Fe(III)	0.50	1.05	
MMO, Me. trichosporium	Fe1(II)–Fe2(II)	1.3	3.1	50
		1.3	2.4–3.0	
	Fe1(III)–Fe2(III)	0.51	1.16	
		0.5	0.87	
FeZSM-5 (after contacting wet air)	Fe(II)–Fe(II)	1.36	3.21	This work
	Fe(III)–Fe(III)	0.47	0.96	

oxidized states active iron parameters in FeZSM-5 coincide with those in MMO. This provides additional evidence for the dinuclear structure of active iron complexes in zeolites and explains the remarkable analogy between the chemical properties of α-oxygen and active oxygen of MMO described in a number of works (5, 51, 52).

Recently, using EXAFS techniques, Prins and coworkers (41) also found in FeZSM-5 zeolites iron complexes similar to active sites in MMO.

4.3. Nuclearity of α-Sites

Note that an α-site is an iron entity able to adsorb one atom of α-oxygen. This definition serves as a basis for experimental measurements of α-site concentrations via N_2O decomposition by reaction [1]. Both present and previous Mössbauer results reliably show that α-sites are related to dinuclear iron complexes. On this ground we used to assume (5, 52) that such a dinuclear complex formed one α-site. But more thorough consideration implies that this conclusion would be valid if such a complex adsorbs only one atom of α-oxygen. However, we cannot rule out that *each Fe atom* in the complex may adsorb α-oxygen. This would mean that α-sites are mononuclear species, although they compose dinuclear complexes.

One may solve the problem of α-site nuclearity by quantitatively comparing the concentration of Fe active atoms able to redox transitions with that of α-sites:

$$n_\alpha = C_{\mathrm{Fe_{act}}}/C_\alpha. \qquad [3]$$

Our experimental results allow us to estimate the value of n_α by several methods (Table 8). First the value $n_\alpha = 1.5$ in Table 8 is found directly from the linear relationship between the summed concentration of Fe^{2+} (D3 + D4) versus that of α-sites (Fig. 4c). However, this value is obviously overestimated. From Table 3 (sample 5) and Table 4 (samples 6 and 7), one may see that on average ca. 30% of bivalent iron is not involved, for some reason, in the α-oxygen loading. Appropriate correction gives $n_\alpha \approx 1.0$.

Other estimates in Table 8 are based on the results of α-oxygen loading onto vacuum- and steam-activated samples. This allows immediate comparison between the number of iron atoms which experienced $Fe^{2+} \rightarrow Fe^{3+}$ oxidation and the number of O_α atoms causing this transformation. O_α loading into FeZSM-5 (A) (Table 3, sample 4 $\rightarrow$ sample 5) gives $n_\alpha = 1.1$. The value of n_α for FeZSM-5 (B) after vacuum activation (Table 4, sample 4 $\rightarrow$ sample 6) is 1.2 and after steam activation (Table 4, sample 5 $\rightarrow$ sample 7) is 0.9. Therefore, one atom of active iron adsorbs one atom of O_α. It means that each dinuclear complex consists of two α-sites.

Regarding the obtained results, we may propose the following qualitative model of α-site formation. When iron is introduced at the stage of zeolite synthesis, Fe^{3+} atoms initially occupy the tetrahedral positions of the crystalline lattice. At high-temperature activation, due to the presence of defects, iron atoms migrate over the crystal and may move from the lattice into the micropore space, forming dinuclear complexes stabilized at the charge compensating sites (53). This removal is accompanied by oxygen loss, and by complex I transition to complex II, producing two α-sites represented by two Fe^{2+} atoms, as shown schematically in Fig. 8. Due to lattice relaxation and environment rearrangement, atoms Fe^{2+} in complex II acquire a new stable state so that their reverse oxidation by O_2 becomes impossible. However, Fe^{2+} can be easily oxidized to Fe^{3+} by α-oxygen adsorption yielding complex III. The exactly reversible $Fe^{2+} \leftrightarrow Fe^{3+}$ transition ensures a smooth α-oxygen transfer from N_2O to organic molecules, thus providing FeZSM-5 with selective oxygenation properties (4, 7). Catalytic N_2O decomposition with evolution of N_2 and O_2 also proceeds due to this transition.

Complex I in Fig. 8 has a structure similar to that proposed by Prins and coworkers (41). Unlike other dinuclear complexes discussed in the literature, this complex includes a μ-hydroxogroup and, therefore, may have an overall monopositive charge suitable for compensating the charge of the zeolite lattice induced by a single Al atom. This increases the probability that such complexes exist, since for their formation there is no need for two neighboring Al atoms in the lattice. Estimates made in (54, 55) show that the probability of such Al pairs occurring in the high-silica zeolites is very small.

Note that the mononuclear structure of α-sites discovered in this work assumes α-oxygen to be a negative O^- species with an unpaired electron. The electronic state of

TABLE 8

Evaluation of α-Site Nuclearity

Evaluation method	From Fig. 4c		From loading of α-oxygen		
	Direct value	Corrected value	FeZSM-5 (A), vacuum activation	FeZSM-5 (B)	
				Vacuum activation	Steam activation
Nuclearity, n_α (Fe/α-site)	1.5	~1.0	1.1	1.2	0.9

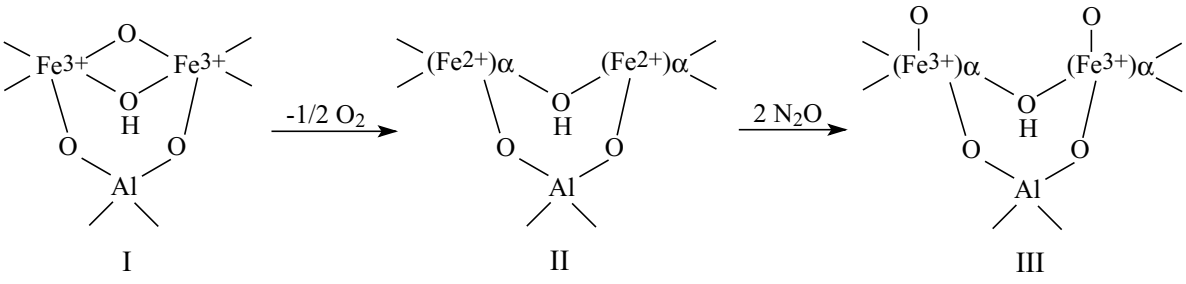

FIG. 8. Formation of a pair of α-sites in the form of a dinuclear iron complex.

α-oxygen is discussed in detail in a separate paper including new data obtained recently on this challenging subject (57).

5. CONCLUSIONS

Many recent studies relate to the iron state in zeolites. However, only a few of them directly focus on the identification of active iron composing α-sites. In this state, iron is able to decompose nitrous oxide, with the adsorption of α-oxygen providing unique oxidation properties to Fe-containing zeolites.

Our previous Mössbauer studies indicate that α-oxygen formation is related to the presence of dinuclear Fe complexes. In the present work, we for the first time made a thorough quantitative comparison of adsorption, catalytic, and Mössbauer data *in situ* obtained for FeZSM-5 samples subjected to stepwise activation. This study shows that active iron actually exists in the form of dinuclear complexes. As a somewhat unexpected result, it turns out that each atom in the complex is capable of generating α-oxygen. It means that α-sites are monatomic entities in a paired arrangement registered by Mössbauer spectroscopy as dinuclear complexes.

Such a paired arrangement of α-sites agrees with the mechanism of room temperature methane interaction with α-oxygen. According to IR data (56), this interaction proceeds via methane dissociation yielding hydroxy and methoxy groups. It is noteworthy that both groups include α-oxygen atoms, which seems to be an obvious result for this type arrangement.

The catalytic significance of paired dispositions of α-sites is not clear. It may be an indifferent phenomenon not important for single-site functioning. But remembering the dinuclear structure of iron active sites in MMO, one may also assume the paired arrangement of α-sites to be of fundamental significance for generating extraordinarily active α-oxygen species. The present paper suggests no answer to this question, which is worth a special study.

ACKNOWLEDGMENTS

We thank Dr. L. Pirutko for zeolite synthesis. Coauthors from the Boreskov Institute of Catalysis thank Solutia Inc. for financial support and permission to publish these data. A. A. Sh. thanks INTAS (Grant 97-1289) and U.S. Civilian Research and Development Foundation (CRDF, Grant RC1-2058) for financial support.

REFERENCES

1. Centi, G., Wichterlowa, B., and Bell, A., Eds., "Catalysis by Unique Metal Ion Structures in Solid Matrices," NATO Science Series. Kluwer Academic, Dordrecht/Norwell, MA, 2001.
2. Panov, G. I., Kharitonov, A. S., and Sobolev, V. I., *Appl. Catal.* **98**, 1 (1993).
3. Ovanesyan, N. S., Shteinman, A. A., Sobolev, V. I., Dubkov, K. A., and Panov, G. I., *Kinet. Katal.* **39**, 863 (1998).
4. Rodkin, M. A., Sobolev, V. I., Dubkov, K. A., Watkins, N. H., and Panov, G. I., *Stud. Surf. Sci. Catal.* **130**, 875 (2000).
5. Panov, G. I., Sobolev, V. I., Dubkov, K. A., Parmon, V. N., Ovanesyan, N. S., Shilov, A. E., and Shteinman, A. A., *React. Kinet. Catal. Lett.* **61**, 251 (1997).
6. Panov, G. I., Uriarte, A. K., Rodkin, M. A., and Sobolev, V. I., *Catal. Today* **41**, 365 (1998).
7. Panov, G. I., *Cattech* **4**, 18 (2000).
8. Uriarte, A. K., Rodkin, M. A., Gross, M. J., Kharitonov, A. S., and Panov, G. I., *Stud. Surf. Sci. Catal.* **110**, 857 (1997).
9. Filatov, M. J., Pelmenschikov, A. G., and Zhidomirov, G. M., *J. Mol. Catal.* **8**, 243 (1993).
10. Yoshizawa, K., Shiota, Y., Yumura, T., and Yamabe, T., *J. Phys. Chem. B* **104**, 734 (2000).
11. Sobolev, V. I., Dubkov, K. A., Paukshtis, E. A., Pirutko, L. V., Rodkin, M. A., Kharitonov, A. S., and Panov, G. I., *Appl. Catal. A* **141**, 185 (1996).
12. Argauer, R. J., and Landolt, G. R., U.S. Patent 3,702,886, assigned to Mobile Oil Co. (1972).
13. Panov, G. I., Sobolev, V. I., and Kharitonov, A. S., *J. Mol. Catal.* **61**, 85 (1990).
14. Dubkov, K. A., Sobolev, V. I., and Panov, G. I., *Kinet. Katal.* **39**, 79 (1998).
15. Ribera, A., Arends, I. W. C. E., de Vries, S., Perez-Ramirez, J., and Sheldon, R. A., *J. Catal.* **195**, 287 (2000).
16. Zecchina, A., and Berlier, G., *in* "Catalysis by Unique Metal Ion Structures in Solid Matrices" (G. Centi, B. Wichterlowa, and A. Bell, Eds.), NATO Science Series, p. 135. Kluwer Academic, Dordrecht/Norwell, MA, 2001.
17. Sobolev, V. I., Panov, G. I., Kharitonov, A. S., Romannikov, V. N., Volodin, A. M., and Ione, K. G., *J. Catal.* **139**, 435 (1993).
18. Kharitonov, A. S., Sheveleva, G. A., Panov, G. I., Sobolev, V. I., Paukshtis, Y. A., and Romannikov, V. N., *Appl. Catal. A* **98**, 33 (1993).
19. Pirutko, L. V., Chernyavsky, V. S., Uriarte, A. K., and Panov, G. I., *Microporous Mesoporous Mater.* **48**, 345 (2001).
20. Meagher, A., Nair, V., and Szostak, R., *Zeolites* **8**, 3 (1988).
21. Garten, R. L., Delgass, W. N., and Boudart, M., *J. Catal.* **19**, 90 (1970).

22. Kurts, D. M., Jr., *Chem. Rev.* **90**, 585 (1990).
23. Segawa, K. I., Chen, Y., Kubsh, J. E., Delgass, W. N., Dumesic, J. A., and Hall, W. K., *J. Catal.* **76**, 112 (1982).
24. Lazar, K., Borbely, G., and Beyer, H., *Zeolites* **11**, 214 (1991).
25. Debrunner, P. G., *Hyperfine Interact.* **53**, 21 (1990).
26. Gutlich, P., and Ensling, J., *in* "Inorganic Electronic Structure and Spectroscopy" (E. I. Solomon and A. B. P. Lever, Eds.), Vol. 1, p. 161. Wiley, New York, 1999.
27. Rethwisch, D. G., and Dumesic, J. A., *J. Phys. Chem.* **90**, 1863 (1986).
28. Menage, S., Zang, Y., Hendrich, M. P., and Que, L., Jr., *J. Am. Chem. Soc.* **114**(20), 7786 (1992).
29. Lazar, K., Kotasthane, A. N., and Fejes, R., *Catal. Lett.* **57**, 171 (1999).
30. Mauvezin, M., Delahay, G., Coq, B., Kieger, S., Jumas, J. C., and Oliver-Fourcade, J., *J. Phys. Chem. B* **105**, 928 (2001).
31. Coq, B., Mauvezin, M., Delahay, G., and Kieger, S., *J. Catal.* **195**, 298 (2000).
32. Fejes, P., Nagy, J. B., Lazar, K., and Halasz, J., *Appl. Catal. A* **190**, 117 (2000).
33. Lazar, K., Lejeune, G., Ahedi, R. K., Shevade, S. S., and Kotasthane, A. N., *J. Phys. Chem. B* **102**, 4865 (1998).
34. Feng, X., and Hall, W. K., *J. Catal.* **166**, 368 (1997).
35. Chen, H.-Y., and Sachtler, W. M. H., *Catal. Today* **42**, 73 (1998).
36. Knops-Gerrits, P. P., Van Bavel, A.-M., Liangouche, G., and Jacobs, P. A., in "Catalytic Activation and Functionalization of Light Alkanes" (E. G. Derouane, *et al.*, Eds.), p. 215. Kluwer Academic, Dordrecht/Norwell, MA, 1998.
37. Mizuno, N., Kiyoto, I., Nozaki, Ch., and Misono, M., *J. Catal.* **181**, 171 (1999).
38. Callis, G., and Frenken, P., *Zeolites* **7**, 319 (1987).
39. Kucherov, A. V., and Slinkin, A. A., *Zeolites* **8**, 110 (1988).
40. Voskoboinikov, T. V., Chen, H.-Y., and Sachtler, W. M. H., *Appl. Catal. B* **19**, 279 (1998).
41. Marturano, P., Drozdova, L., Kogelbauer, A., and Prins, R., *J. Catal.* **192**, 236 (2000).
42. Battiston, A. A., Bitter, J. H., and Koningsberger, D. C., *Catal. Lett.* **66**, 75 (2000).
43. Ding, X.-Q., Bominaar, E. L., Bill, E., Winkler, H., Trautwein, A. X., Drueke, S., Chaudhuri, P., and Wieghardt, K., *Hyperfine Interact.* **53**, 311 (1990).
44. Petrera, M., Gennaro, A., Gherardi, P., Gubitosa, G., and Pernicone, N., *J. Chem. Soc., Faraday Trans.* **1**(80), 709 (1984).
45. Broadwater, J. A., Achim, C., Fox, B. G., Munck, E., and Que, L., Jr., *J. Biol. Inorg. Chem.* **3**, 392 (1998).
46. Spoto, G., Zecchina, A., Berlier, G., Bordiga, S., Clerici, M. G., and Basini, L., *J. Mol. Catal. A* **158**, 107 (2000).
47. Dumesic, J. A., Fang, S. M., Long, M. A., Ulla, M. A., Millman, W. S., and Hall, W. K., *J. Catal.* **104**, 381 (1987).
48. Lobree, L. J., Hwang, I., Reimer, J. A., and Bell, A. T., *J. Catal.* **186**, 242 (1999).
49. Joyner, R., and Stockenhuber, M., *J. Phys. Chem. B* **103**, 5963 (1999).
50. Wallar, B. J., and Lipscomb, J. D., *Chem. Rev.* **96**, 2625 (1996).
51. Dubkov, K. A., Sobolev, V. I., Talsi, E. P., Rodkin, M. A., Watkins, N. H., Shteinman, A. A., and Panov, G. I., *J. Mol. Catal.* **123**, 155 (1997).
52. Panov, G. I., Sobolev, V. I., Dubkov, K. A., and Kharitonov, A. S., *Stud. Surf. Sci. Catal.* **101**, 493 (1996).
53. Pirutko, L. V., Chernyavsky, V. S., Uriarte, A. K., and Panov, G. I., *Appl. Catal.*, in press.
54. Feng, X., and Hall, W. K., *Catal. Lett.* **46**, 11 (1997).
55. Rice, M. J., Chakraborty, A. K., and Bell, A. T., *J. Catal.* **186**, 222 (1999).
56. Panov, G. I., Dubkov, K. A., and Paukshtis, Ye. A., *in* "Catalysis by Unique Metal Ion Structures in Solid Matrices" (G. Centi, B. Wichterlowa, and A. Bell, Eds.), NATO Science Series, p. 149. Kluwer Academic, Dordrecht/Norwell, MA, 2001.
57. Dubkov, K. A., Starokon, E. V., Shteinman, A. A., and Panov, G. I., manuscript in preparation.